TECNIACUSTICA ELCHE · 2022

53º CONGRESO ESPAÑOL DE ACÚSTICA
XII CONGRESO IBÉRICO DE ACÚSTICA

MFree Local Weak-Form Cumulant Lattice Boltzmann Methods: Aeroacoustic Consideration

PACS: 02.70.-c, 43.58.Ta, 45.10.-b, 46.15.-x, 47.35.Rs.

Gorakifard, Mohsen[1]; Salueña, Clara[1]; Cuesta, Ildefonso[1]; Kian Far, Ehsan[2]

1 Rovira i Virgili University.
Tarragona. Spain.
Email: mohsen.goraki@urv.cat
2 Siemens Digital Industries Software.
Nottingham. United Kingdom.

Palabras Clave: MFree, Local weak-form, Cumulant lattice Boltzmann, Aeroacoustic

ABSTRACT.
The Lattice Boltzmann Method (LBM) has shown robustness in simulating wave propagation. However, this method suffers from issues of accuracy and computational efficiency related to the use of uniform meshes. Therefore, two MFree (meshfree) local weak-form cumulant LB methods are suggested to overcome these shortcomings: the local radial point interpolation cumulant LBM (LRPIC-LBM) and the meshless local Petrov-Galerkin cumulant LBM (MLPGC-LBM). The collision step of LBM is modeled by the cumulant method, while the streaming step is, first, discretized in time using the Lax-Wendroff scheme, then, the space discretization is done by means of the local radial point interpolation method (RPIM) and the meshless local Petrov-Galerkin method (MLPG) -for LRPICLBM and MLPGC-LBM, respectively. To substantiate the accuracy of these methods the propagation of planar acoustic waves is studied, comparing the results from the LBM simulations with their respective analytical solutions. The comparisons illustrate that both MFree local weak-form cumulant LB methods replicate the analytical results, and even improve those of the LBM. Therefore, both new methods offer an interesting alternative to conventional LBM methods, with the relevant feature that they are not penalized by the parametric dependence of the number of points per wavelength.

RESUMEN.
El método Lattice Boltzmann (LBM) ha demostrado su solidez en la simulación de la propagación de ondas. Sin embargo, este método adolece de problemas de precisión y eficiencia computacional relacionados con el uso de mallas uniformes. Por lo tanto, se sugieren dos métodos LBM-MFree de forma local débil para superar estas deficiencias: el LBM de interpolación local de puntos radiales (LRPIC-LBM) y el LBM cumulante de Petrov-Galerkin local sin malla (MLPGC-LBM). El paso de colisión del LBM se modela mediante el método cumulante, mientras que el paso de propagación es primero discretizado en el tiempo utilizando el esquema de Lax-Wendroff, y luego la discretización en el espacio se realiza mediante el método local de interpolación de puntos radiales (RPIM) y el método local de Petrov-Galerkin sin malla (MLPG) -para el LRPICLBM y el MLPGC-LBM, respectivamente. Para corroborar la precisión de estos métodos se estudia la propagación de ondas acústicas planas comparando los resultados de las simulacions LBM con sus respectivas soluciones analíticas. Las comparaciones ilustran que ambos métodos LB-MFree replican los resultados analíticos, e incluso mejoran los del LBM convencional. Por tanto, ambos nuevos métodos ofrecen una interesante alternativa a los métodos LBM convencionales, con la relevante característica de que no se ven penalizados por la dependencia paramétrica del número de puntos por longitud de onda.

1. INTRODUCCIÓN

The sound propagation as one of the crucial issues [1], not only affects many industries by limiting engine operation and polluting the environment, but also makes engineering modeling complicated, particularly for the need of enormous CPU-time and robustness of algorithms. Projects and research centers have been launched that focus on suitable computational aeroacoustic (CAA) implementations [2]. For these purposes, various schemes have been concocted in computational aeroacoustics. Tam [3] and Wells et al. [4] suggested compact and non-compact optimized schemes like the High-order Compact Difference scheme and the Dispersion-relation-preserving (DRP) scheme. Hybrid methods were also adopted to slash the huge cost of CAA simulations [5].

However, factors like the small ratio between sound pressure and pressure variation and the time-consuming nature of the traditional methods make direct simulation of aerostatics challenging [6]. Thus, the LBM have been devised to simulate sound wave propagation due to their relative simplicity of implementation and parallelization. Dellar et al. [7] reached acceptable results for sound wave propagation using LBM. Bres et al. [8] and Gorakifard et al. [9] considered the dissipation and dispersion of acoustic waves using the BGK and the cumulant LBM, respectively. A regularized method for the BGK-LBM [10] has been developed to model wave propagation.

In general, the LBM is constrained by lattice uniformity so it suffers from accuracy and efficiency problems in non-uniform mesh simulations [11]. Although grid refinement can improve accuracy, it favors the appearance of additional perturbations in acoustics [12]. To overcome these weaknesses, non-uniform LB methods have been developed such as: interpolation-supplemented LBM [13], combinations of LBM with finite difference/ volume/ element methods [14], and Taylor-series expansion and least-squares-based lattice Boltzmann methods [15]. These methods suffer from the drawbacks caused by meshes, such as mesh generation costs, low accuracy of calculated stresses in fluid-structure interaction simulations [16], and simulation failure for singular physical phenomena. Thus, Mesh-Free methods were presented to encounter above problems. These methods generate a system of algebraic equations for the nodes, without explicit linkage among them to interpolate or approximate the unknown variables.

MFree methods have developed along with older methods like the collocation method [18] and the vortex method [19]. Among the so-called weak-form MFree methods, different procedures have aroused the interest of researchers in computational mechanics. These methods include the local radial point interpolation method (LRPIM) [20] and the meshless local Petrov-Galerkin method (MLPG) [21]. Mfree methods in LBM have also been used with success in fluid flow simulations [22]. However, such idea is still at an early stage of development and must be improved. As an illustration, studies using the standard Bhatnagar-Gross-Krook (BGK) scheme in the collision part, suffer from instability at low viscosities, and violation of the principle of Galilean invariance [23]. Thus, replacing the BGK scheme by the more stable cumulant LBM [24, 25] provides premium advantages. For this purpose, the local radial point interpolation cumulant lattice Boltzmann method (LRPIC-LBM) [26] has been developed. Moreover, the efficiency of LRPIC-LBM increases by using MLPG in the Mfree part, since the moving least squares (MLS) shape functions used in MLPG need less computational resources than the RPIM shape functions used in LRPIM. This idea has resulted in the meshless local Petrov-Galerkin cumulant LB method (MLPGC-LBM) [27]. The main aim of this study is to assess the ability of two MFree local weak-form cumulant LB methods: the local radial point interpolation cumulant LBM (LRPIC-LBM) and the meshless local Petrov-Galerkin cumulant LBM (MLPGC-LBM) to simulate aeroacoustics problems.

2. THE LATTICE BOLTZMANN METHOD

The lattice Boltzmann method (LBM) originated from the kinetic theory of gases [28]. The lattice Boltzmann equation without an external force is

$$f_i\left(x + c_i\Delta t, t + \Delta t\right) - f_i\left(x, t\right) = \Omega_i \tag{1}$$

where x and c_i are vectors of the position and lattice speed, f_i is the particle distribution function and Ω_i is the collision operator.

In general, the LBM is comprised of collision and streaming steps. In MFree local weak-form cumulant LB methods, the cumulant method is used for the collision part. For the streaming part, we will use the local radial point interpolation method (RPIM) in the case of the LRPIC-LBM, and the meshless local Petrov-Galerkin method for the MLPG-CLBM.

2.1. Collision Step

The cumulant LBM has been suggested to solve the Boltzmann equation [29]. It can improve the cascade LBM [30]. The central moments can efficiently be described by the cumulants of a distribution function. The cumulants are calculated as

$$c_{\zeta^m\psi^n} = \frac{\partial^m \partial^n}{\partial \mathrm{Z}^m \partial \Psi^n} \ln\left(M\left(\mathrm{Z},\Psi\right)\right)\Big|_{\mathrm{Z}=\Psi=0} \tag{2}$$

where M is the moment generating function and Z,Ψ are the normalized wave numbers. The cumulants relax with individual relaxation rates [31],

$$c^*_{\zeta^m\psi^n} = c_{\zeta^m\psi^n} + \omega_{\zeta^m\psi^n}\left(c^{eq}_{\zeta^m\psi^n} - c_{\zeta^m\psi^n}\right) \tag{3}$$

where Z,Ψ are the equilibrium state cumulants [32].

2.2. Streaming Step

In general, to model the streaming part, a pure advection equation is solved by a Lagrangian approach within uniform structured meshes. By shifting to the Eulerian perspective, it is possible to overcome uniform structured meshe problems. The pure advection equation is

$$\frac{\partial f_i}{\partial t} + c_{i,\alpha}\frac{\partial f_i}{\partial x_\alpha} = 0 \tag{4}$$

Equation (4) is discretized based on a semi-discrete formulation. Therefore, the Lax–Wendroff scheme, for time, and the local radial point interpolation method (RPIM) and the meshless local Petrov-Galerkin method (MLPG), for space discretization are separately used.

2.2.1. Mfree shape function construction - Radial point interpolation shape functions

Radial point interpolation method (RPIM) shape functions were suggested to overcome the singularity issues. The RPIM interpolation augmented with polynomials is

$$f^h\left(\mathbf{x},t\right) = \sum_{i=1}^{n} R_i\left(\mathbf{x}\right)a_i\left(t\right) + \sum_{j=1}^{m} p_j\left(\mathbf{x}\right)b_j\left(t\right) = \mathbf{R}^T\left(\mathbf{x}\right)a\left(t\right) + \mathbf{p}^T\left(\mathbf{x}\right)\mathbf{b}\left(t\right) \tag{5}$$

where $R_i\left(\mathbf{x}\right)$ is a radial basis function (RBF), and $p_j\left(\mathbf{x}\right)$ is monomial in the coordinate space and $x^T = \left[x, y\right] : \mathbf{R}^T = \left[R_1\left(\mathbf{x}\right)R_2\left(\mathbf{x}\right)\cdots R_n\left(\mathbf{x}\right)\right]$. Parameters n and m are the number of RBFs and polynomial basis functions. Variables a_i and b_j are time dependent unknown coefficients. Moreover, the independent variable in RBF $R_i\left(x\right)$ is the distance between the point of interest x and a node at x_i.

Using some specific constraint equations, the approximation function can be calculated

$$f^h\left(\mathbf{x},t\right) = \sum_{i=1}^{n} \phi_i\left(\mathbf{x}\right)f_i\left(t\right) = \mathbf{\Phi}\left(\mathbf{x}\right)\mathbf{F}\left(t\right) \tag{6}$$

where $\mathbf{F}$ is a vector containing the nodal values of the distribution function and $\mathbf{\Phi}$ is a vector containing the first n components of the $\tilde{\mathbf{\Phi}} = \left[\mathbf{R}^T\ \mathbf{p}^T\right]\mathbf{G}^{-1}$ vector

$$\mathbf{G}=\begin{bmatrix}\mathbf{R}_0 & \mathbf{P}_m\\ \mathbf{P}_m^T & 0\end{bmatrix},\mathbf{R}_0=\begin{bmatrix}R_1(r_1) & R_2(r_1) & \cdots & R_n(r_1)\\ R_1(r_2) & R_2(r_2) & \cdots & R_n(r_2)\\ \vdots & \vdots & \ddots & \vdots\\ R_1(r_n) & R_2(r_n) & \cdots & R_n(r_n)\end{bmatrix} \tag{7}$$

2.2.2. Mfree shape function construction - Moving least squares shape functions

In the moving least squares (MLS) approximation, the distribution function is approximated by

$$f(\mathbf{x},t)\approx f^h(\mathbf{x},t)=\sum_{i=1}^{m}p_i(\mathbf{x})a_i(\mathbf{x},t)=\mathbf{p}^T(\mathbf{x})\mathbf{a}(\mathbf{x},t) \tag{8}$$

where m , $p_i(x)$ and $a_i(x,t)$ are the number of basis functions, the basis functions, and their corresponding coefficients, respectively. The coefficient $\mathbf{a}$ is calculated by minimizing the difference between the local approximation and the function which yields

$$\mathbf{A}(\mathbf{x})\mathbf{a}(\mathbf{x},t)=\mathbf{B}(\mathbf{x})\mathbf{F}(t) \tag{9}$$

where

$$\mathbf{A}(\mathbf{x})=\sum_{i=1}^{n}w_i\mathbf{p}(\mathbf{x}_i)\mathbf{p}^T(\mathbf{x}_i)=\begin{bmatrix}\sum_{i=1}^{n}w_i & \sum_{i=1}^{n}x_iw_i & \sum_{i=1}^{n}y_iw_i\\ \sum_{i=1}^{n}x_iw_i & \sum_{i=1}^{n}x_i^2w_i & \sum_{i=1}^{n}x_iy_iw_i\\ \sum_{i=1}^{n}y_iw_i & \sum_{i=1}^{n}x_iy_iw_i & \sum_{i=1}^{n}y_i^2w_i\end{bmatrix}$$

$$\mathbf{B}(\mathbf{x})=\left[w_1(\mathbf{x})\mathbf{p}(\mathbf{x}_1),w_2\mathbf{p}(\mathbf{x}_2),\cdots,w_n\mathbf{p}(\mathbf{x}_n)\right]=\begin{bmatrix}w_1 & w_2 & \cdots & w_n\\ x_1w_1 & x_2w_2 & \cdots & x_nw_n\\ y_1w_1 & y_2w_2 & \cdots & y_nw_n\end{bmatrix}$$

$$\mathbf{F}(t)=\left[f_1(t),f_2(t),\cdots,f_n(t)\right]^T \tag{10}$$

estimating $\mathbf{a}(x,t)$ from equation (9), and substituting it into equation (8), yields

$$f^h(\mathbf{x},t)=\sum_{i=1}^{n}\phi_i(\mathbf{x})f_i(t)=\mathbf{\Phi}(\mathbf{x})\mathbf{F}(t) \tag{11}$$

where $\mathbf{\Phi}^T(\mathbf{x})=\mathbf{p}^T(\mathbf{x})\mathbf{A}^{-1}(\mathbf{x})\mathbf{B}(\mathbf{x})$ and the shape function ϕ_i for the i-th node is $\phi_i(\mathbf{x})=\mathbf{p}^T(\mathbf{x})\left(\mathbf{A}^{-1}\mathbf{B}\right)_i$.

2.2.3. Semi-Discrete Formulation - Time discretization

Starting from the Taylor series expansion of the particle distributions and surrogating the time derivatives with the spatial derivatives up to second order, the time discretization of equation (4) based on the Lax-Wendroff scheme is

$$f_i^{n+1}=f_i^n-\Delta tc_{i,\alpha}\frac{\partial f_i^n}{\partial x_\alpha}+\frac{\Delta t^2}{2}c_{i,\alpha}c_{i,\beta}\frac{\partial^2 f_i^n}{\partial x_\alpha\partial x_\beta} \tag{12}$$

2.2.4. Semi-Discrete Formulation - Space discretization

Two MFree local weak-form methods, the local radial point interpolation method (LRPIM), and the meshless local Petrov-Galerkin (MLPG) method are proposed to avert global background cells for either function approximation or integration. In these methods, the numerical integration is carried out within the local domain consisting of a set of distributed nodes. The LRPIM and MLPG are based on the RPIM and the MLS shape functions, respectively, where LRPIM benefits from the delta function property. However, the MLS improves the efficiency of the scheme beyond that of the LRPM. The weighted residual statement of equation (12) on the local domain Ω_I of point I bounded by Γ_I is

$$\int_{\Omega_I} V_I f_i^{n+1} d\Omega = \int_{\Omega_I} V_I f_i^{n} d\Omega - \Delta t \int_{\Omega_I} V_I c_{i,\alpha} \frac{\partial f_i^{n}}{\partial x_\alpha} d\Omega + \frac{\Delta t^2}{2} \int_{\Omega_I} V_I c_{i,\alpha} \frac{\partial^2 f_i^{n}}{\partial x_\alpha \partial x_\beta} d\Omega \qquad (13)$$

where V_I is the local weight function of node I used for the cubic spline function. Using integration by parts and substitution of the approximate solution (6) and (11) into equation (13) plus solving the global equation system separately for each direction yields

$$\mathbf{M} f_i^{n+1} = \left[\mathbf{M} + \mathbf{K}_i\right] f_i^{n} \qquad (14)$$

where f_i, $\mathbf{M}$ and $\mathbf{K}$ are the particle distribution vector, the global mass matrix, and stiffness matrix, respectively.

3. RESULTS AND DISCUSSION

Aeroacoustics has recently adopted the LBM due to reduced computational costs. For a standard aeroacoustic analysis, properties of planar acoustic waves will be studied using two MFree local weak-form cumulant LB methods. For this purpose, the temporal decay of a standing plane wave in a periodic domain is considered for regular (default) and irregular nodal distributions (shown in Figures 1a and 1b). The base units are in the LB system. The assumptions for this set-up are those of reference (33) for ease of comparison. The results of the temporal analysis will be presented as a function of the number of points per wavelength $N_{ppw} = \lambda / \Delta x$.

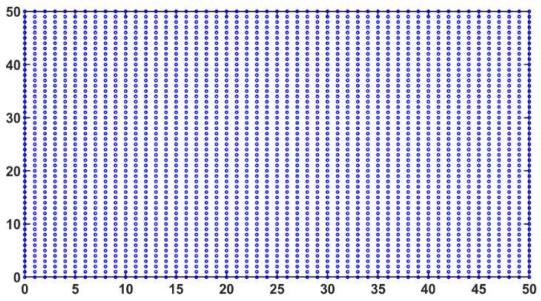

(A) Regular nodes.

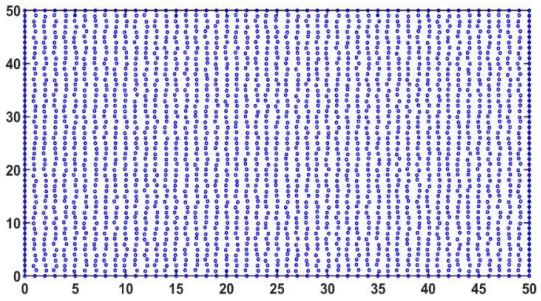

(B) Irregular nodes.

Figura 1 – Nodal arrangement for the propagation of planar acoustic waves.

The relative numerical error of the phase speed for the cumulant LBM is depicted as a function of the non-dimensional wave-number in Figure 2. It shows that the deviations from the theoretical values are small, for a resolution with more than 12 points per wavelength; for example, at 12 points per wavelength these deviations are about 0.77% in the phase speed. Furthermore and as in reference [9], a reduction in viscosity does not have effects on the phase speed, which allows us to conclude that the results are only a function of N_{ppw} (number of points per wavelength) and are independent of viscosity in the range of interest. However, reducing the resolution increases the errors, and it would be desirable if the results were independent of the number of points per wavelength. Figure 3 shows the acoustic pressure time history for $\nu = 1.0\times10^{-2}\left[\Delta x^2/\Delta t\right]$ with N_{ppw}=12. The LRPIC-LBM exhibits very good agreement with the analytical acoustic pressure.

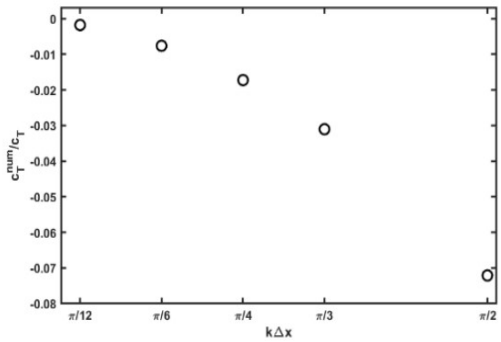

Figura 2 – Relative numerical error of the phase speed for the cumulant LBM as a function of the non-dimensional wave-number.

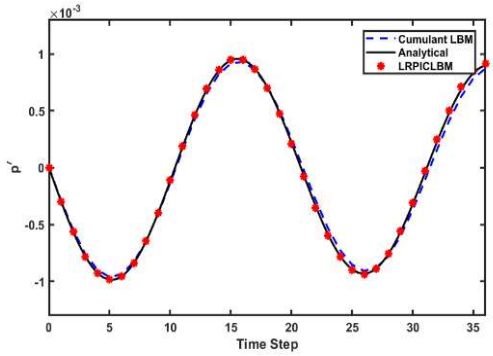

Figura 3 – Acoustic pressure vs. time for $\nu = 1.0\times10^{-2}$ and N_{ppw}=12.

The acoustic pressure time history for a viscosity 100 times smaller $\nu = 1.0\times10^{-4}\left[\Delta x^2/\Delta t\right]$ with N_{ppw}=12 is shown in Figure 4. It presents the comparison between the analytical solution, the cumulant LBM and the LRPIC-LBM numerical solutions at low viscosities. The typical instability seen in the BGK LBM at low viscosities is avoided by using the cumulant LBM, with phase speed errors of less than 1 percent, with adequate resolution. The LRPIC-LBM exhibited good performance, closely following the theoretical result. Based on figure 2, the error for N_{ppw}=4 is more than 7% for the cumulant LBM. However for the LRPIC-LBM, the acoustic pressure time history for N_{ppw}=4 and $\nu = 1.0\times10^{-2}\left[\Delta x^2/\Delta t\right]$ presented in Figure 5 reveals that the deviation is less than 2%, with a the time step value of Dt = 0.25. The time step size has effects on the accuracy and stability of the solution. To reduce errors, the time step can be reduced.

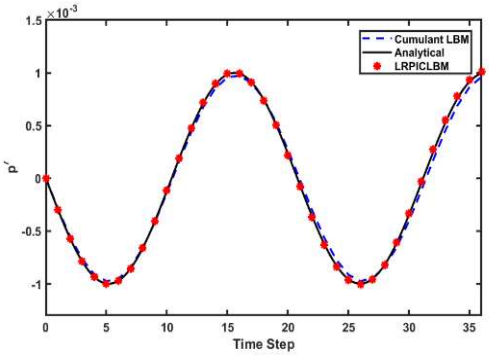

Figura 4 – Acoustic pressure vs. time for $\nu = 1.0\times10^{-4}$ and N_{ppw}=12.

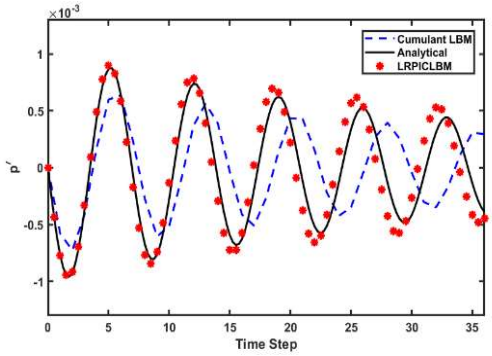

Figura 5 – Acoustic pressure vs. time for $\nu = 1.0\times10^{-2}$ and N_{ppw}=4 with Dt=0.25.

Figure 6 illustrates the acoustic pressure time history for $\nu = 1.0 \times 10^{-2} \left[\Delta x^2 / \Delta t \right]$ with N_{ppw}=4 and Dt = 0.1. The LRPIC-LBM replicates the analytical results with insignificant errors. Figure 7 repeats the previous comparison for the analytical solution, the meshless local Petrov–Galerkin cumulant lattice Boltzmann method (MLPGC-LBM) with linear and quadric basis functions for the expansion of the distribution functions (section 2.2.2). Although one of the cons of MLPGM is that the Kronecker delta condition is not satisfied, and the accuracy of the results is reduced as a consequence, MLPGC-LBM with linear basis functions is more successful in predicting theoretical results than the cumulant LBM. It shows that increasing the polynomial degree of the basis functions, i.e. replacing linear basis functions with quadric ones, leads to an improvement. Moreover, one of the advantages of MLPGM over LRPIM is its higher efficiency due to the difference in the interpolation procedures (the MLS moving least squares shape functions). For example, the average run time for the MLPGC-LBM is less than one third that of the LRPIC-LBM. In summary, both methods give similar results, predicting wave motion accurately with no dependency on the number of points per wavelength, but with less run time in the case of MLPGC-LBM.

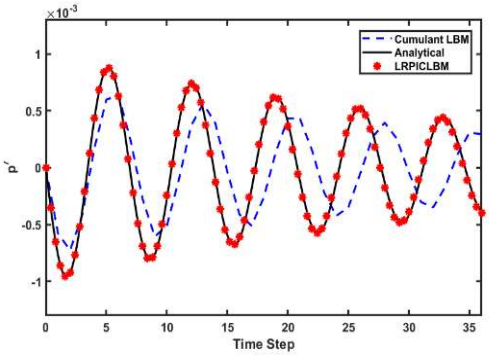

Figura 6 – Acoustic pressure vs. time for $\nu = 1.0 \times 10^{-2}$ and N_{ppw}=4 with Dt=0.1 using LRPIC-LBM.

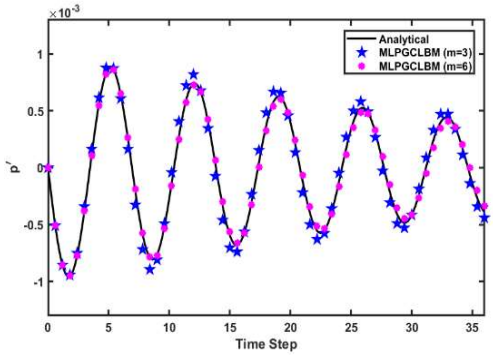

Figura 7 – Acoustic pressure vs. time for $\nu = 1.0 \times 10^{-2}$ and N_{ppw}=4 with Dt=0.1 using MLPGC-LBM.

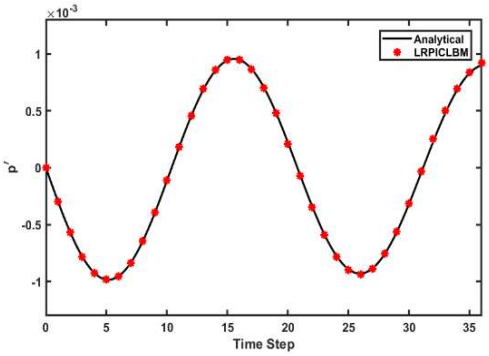

Figura 8 – Acoustic pressure vs. time for irregular nodal distributions using LRPIC-LBM.

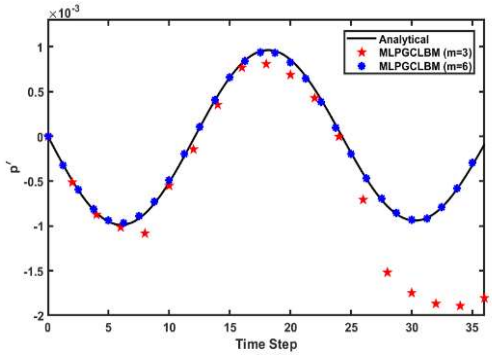

Figura 9 – Acoustic pressure vs. time for irregular nodal distributions using MLPGC-LBM.

In many engineering problems such as those of acoustics, it is necessary to use irregular nodes for simulations in complex geometries. The acoustic pressure time history for $\nu = 1.0 \times 10^{-2} \left[\Delta x^2 / \Delta t \right]$ with N_{ppw}=12 for LRPIC-LBM on the irregular nodal distribution of Figure 1b is presented in Figure 8. It shows that the local radial point interpolation cumulant lattice Boltzmann method (LRPIC-LBM) very closely replicates the analytical acoustic pressure. Similarly, Figure 9 presents the acoustic pressure time history for MLPGC-LBM with N_{ppw}=14 points per wavelength on the same domain and with the same viscosity, determined with linear

basis functions and quadric basis functions. It shows that MLPGC-LBM with linear basis functions cannot model wave motion accurately, due to the lack of a delta function. However, the results of MLPGC-LBM with quadric basis functions dramatically improve and very closely reproduce the analytical acoustic pressure.

4. CONCLUSIONES

This study presents the temporal decay of a standing plane wave using two MFree local weak-form cumulant LB methods: the local radial point interpolation / the meshless local Petrov-Galerkin cumulant LBM. The comparison of the results clarified that the acoustic pressure time history for all three LB methods has a similar behavior at high enough N_{ppw}. In addition, the decrease of the viscosity does not reduce the stability of MFree local weak-form cumulant LB methods due to the advantages of the cumulant method. However, the MLPGC-LBM predicts the same acoustic pressure time history as the LRPIC-LBM but with shorter run times for low N_{ppw}. Furthermore, to yield correct results for the propagation of acoustic waves using MLPGC-LBM with irregular nodal distributions, quadric basis functions are needed due to inaccuracies generated by the lack of delta function properties in the MLPGM scheme. All in all, the possibility to scatter the computational nodes across the domain without additional cost, plus the accuracy and stability achieved by Mfree methods and the cumulant LBM, make MFree local weak-form cumulant LB methods a good alternative to model aeroacoustics.

AGRADECIMIENTOS

We acknowledge the financial support by the Spanish Ministry of Economy, Industry and Competitiveness Research National Agency (under project DPI2016-75791-C2-1-P), by FEDER funds and by Generalitat de Catalunya - AGAUR (under project 2017 SGR 01234).

REFERENCIAS

[1] Geier, M.; Kian Far, E. A sliding grid method for the lattice Boltzmann method using compact interpolation. *The first international workshop on lattice Boltzmann for wind energy*, 2021.

[2] Robinson, M. C.; Hand, M.; Simms, D.; Schreck, S. Horizontal axis wind turbine aerodynamics: three-dimensional, unsteady, and separated flow influences. *tech. rep., National Renewable Energy Lab., Golden, CO (US)*, 1999.

[3] Tam, C. K. Computational aeroacoustics-Issues and methods. *AIAA journal* 33, 1995, 1788–1796.

[4] Wells, V. L.; Renaut, R. A. Computing aerodynamically generated noise. *Annual review of fluid mechanics* 29, 1997, 161–199.

[5] Groschel, E; Schroder, W; Renze, P; Meinke, M; Comte, P. Noise prediction for a turbulent jet using different hybrid methods. *Computers & fluids* 37, 2008,414-426.

[6] Delfs, J.; Bertsch, L.; Zellmann, C.; Rossian, L.; Kian Far, E.; Ring, T.; Langer, S.C. Aircraft noise assessment—from single components to large scenarios. *Energies* 11, 429, 2018.

[7] Dellar, P.J. Bulk and shear viscosities in lattice Boltzmann equations. *Physical review E* 64, 2001, 031203.

[8] Brès, G.; Pérot, F.; Freed, D. Properties of the lattice Boltzmann method for acoustics. *15th AIAA/CEAS aeroacoustics conference (30th AIAA Aeroacoustics Conference)*, 2009, 3395.

[9] Gorakifard, M.; Cuesta, I.; Salueña; C.; Kian Far, E. Acoustic wave propagation and its application to fluid structure interaction using the cumulant lattice Boltzmann method. *Computers & mathematics with applications*, 2021.

[10] Latt, J.; Chopard, B. Lattice Boltzmann method with regularized pre-collision distribution functions. *Math and comp in simulation* 72, 2006, 165–168.

[11] Fard, E.G. A cumulant LBM approach for Large eddy simulation of dispersion microsystems. Ph.D. Thesis, Univ.-Bibl., 2015.

[12] Gorakifard, M.; Salueña, C.; Cuesta, I.; Kian Far, E. Acoustical analysis of fluid structure interaction using the cumulant lattice Boltzmann method. *The 16th international conference for mesoscopic methods in engineering and science* Heriot-Watt University, Edinburgh, Scotland, 2019.

[13] He, X.; Luo, L.S.; Dembo, M. Some progress in lattice Boltzmann method. Part I. nonuniform mesh grids. *Journal of computational physics* 129,1996, 357 –363.

[14] Lee, T.; Lin, C.L. A characteristic Galerkin method for discrete Boltzmann equation. *Journal of computational physics* 171, 2001, 336 –356.

[15] Shu, C.; Niu, X.; Chew, Y. Taylor-series expansion and least-squares based lattice Boltzmann method: two-dimensional formulation and its applications. *Physical review E* 65, 2002, 036708.

[16] Fard, E.G.; Shirani, E.; Geller, Fluid structure interaction with using of lattice Boltzmann method. S. *13th. annual international conference fluid dynamic conference*, 2010.

[17] Liu, G. R.; Gu, Y.T.; An introduction to meshfree methods and their programming. *Springer science & business media*, 2005.

[18] Slater, J.C. Electronic energy bands in metals. *Physical review* 45, 1934, 794.

[19] Chorin, A.J. Numerical study of slightly viscous flow. *Journal of fluid mechanics* 57, 1973, 785–796.

[20] Liu, G.; Gu, Y. A local radial point interpolation method (LRPIM) for free vibration analyses of 2-D solids. *Journal of sound and vibration* 246, 2001, 29– 46.

[21] Atluri, S.N.; Zhu, T. A new meshless local Petrov-Galerkin (MLPG) approach in computational mechanics. *Computational mechanics* 22, 1998, 117–127.

[22] Musavi, S.H.; Ashrafizaadeh, M. Development of a three dimensional meshless numerical method for the solution of the Boltzmann equation on complex geometries. *Computers & fluids* 181, 2019, 236–247.

[23] Kian Far, E.; Geier, M.; Krafczyk, M. Simulation of rotating objects in fluids with the cumulant lattice Boltzmann model on sliding meshes. *Computers & mathematics with applications,* 2018.

[24] Kian Far, E.; Geier, M.; Kutscher, K.; and Konstantin, M. Simulation of micro aggregate breakage in turbulent flows by the cumulant lattice Boltzmann method. *Computers & fluids* 140, 2016, 222 –231.

[25] Kian Far, E.; Langer, S. Analysis of the cumulant lattice Boltzmann method for acoustics problems. *The 13th International conference on theoretical and computational acoustics,* Vienna, Austria, 2017.

[26] Gorakifard, M.; Salueña, C.; Cuesta, I.; Kian Far, E. Analysis of aeroacoustic properties of the local radial point interpolation cumulant lattice Boltzmann method. *Energies* 14, 2021.

[27] Gorakifard, M., Salueña, C., Cuesta, I., & Kian Far, E. The meshless local Petrov–Galerkin cumulant lattice Boltzmann method: strengths and weaknesses in aeroacoustic analysis. *Acta mechanica* 233(4), 2022,1467-1483.

[28] Kian Far, E.; Gorakifard, M.; Fattahi, E. Multiphase phase-field lattice Boltzmann method for simulation of soluble surfactants. *Symmetry* 13.6, 2021, 1019.

[29] Kian Far, E.; Geier, M.; Kutscher, K.; Krafczyk, M. Distributed cumulant lattice Boltzmann simulation of the dispersion process of ceramic agglomerates. *Journal of Computational methods in sciences and engineering* 16, no. 2, 2016, 231-252.

[30] Kian Far, E.; Geier, M.; Kutscher, K.; Krafczyk, Implicit large eddy simulation of flow in a micro-orifice with the cumulant lattice Boltzmann method. *Computation* 5, no. 2, 2017, 23.

[31] Far K. E. Turbulent flow simulation of dispersion microsystem with Cumulant lattice Boltzmann method. *Proceedings of the formula X*, Manchester, UK. 2019 Jun;24.

[32] Far K, Geier M, Krafczyk M. E. A sliding mesh LBM approach for the simulation of the rotating objects. *Proceedings of the 13th international conference for mesoscopic methods in engineering and science*, Hamburg, Germany 2016.

[33] Gorakifard, M. Meshfree methods: Moving beyond the cumulant lattice Boltzmann mpethod Ph.D. Thesis, *Uni URV*, 2022.